Pergamon

Deep-Sea Research I, Vol. 41, No. 3, pp. 485–510, 1994

0967–0637/94 $7.00+0.00

Population dynamics of the planktic foraminifer *Globigerinoides sacculifer* (Brady) from the central Red Sea

JELLE BIJMA*† and CHRISTOPH HEMLEBEN*

(*Received* 11 *May* 1992; *in revised form* 24 *June* 1993; *accepted* 24 *June* 1993)

Abstract—In the central Red Sea the planktic foraminifer *Globigerinoides sacculifer* (Brady) lives in the upper 80 m of the water column and depth preferences for different size classes could clearly be established. Reproduction takes place at full moon, at about 80 m water depth, probably within the chlorophyll maximum. Juveniles ascend in the water column and reach the surface after less than approximately 2 weeks, before they are 100 μm in diameter. Pre-adult stages of *ca.* 200 μm steadily descend within 9–10 days to the reproductive depth. We identify four morphotypes within *G. sacculifer*. On the basis of shape of the last chamber, two basic morphotypes are defined; normalform and sac-like. The relative size of the last chamber determines two further, secondary, morphotypes; kummerform and kummersac, respectively. In terms of earlier classifications, the kummersac morphotype forms an intergrade between kummerform and sac-like. Analysis of size, depth distribution and time of morphotype formation do not demonstrate a distinct relation between the kummersac and one of the primary morphotypes. Kummerform and kummersac formation reach a peak shortly before full moon, whereas the highest frequencies of sac-like chambers are found around new moon. Since formation of these morphotypes leads gametogenesis by 24–48 h, it could indicate that the reproduction of sac-like morphotypes is isolated from the rest. Although additional evidence is required to decide on the taxonomic status of the normalform and the sac-like morphotype, it is tempting to speculate that reproductive isolation over time can play an important role in the process of speciation. The mean and median sizes of the living population and of the flux assemblage differ mainly because of the growth component in the standing stock and differential sedimentation speed of dead and gametogenic specimens. Differences between the flux assemblage and the thanatocoenosis cannot be explained by simple dissolution phenomena.

1. INTRODUCTION

GLOBIGERINOIDES sacculifer (Brady) is a spinose planktic foraminifer that lives in symbiosis with the dinoflagellate *Gymnodinium beii* (SPERO, 1987) and mainly feeds on calanoid copepods (HEMLEBEN *et al.*, 1989). Because of this symbiotic relationship it is distributed in the photic zone. *Globigerinoides sacculifer* dominates many tropical assemblages, especially if the waters are oligotrophic. Although this is one of the most extensively studied

*Institut und Museum für Geologie und Paläontologie, Universität Tübingen, Sigwartstraße 10, D-72076 Tübingen, Germany.

†Present address: Alfred Wegener Institut für Polar- und Meeresforschung, Columbusstrasse, D-27568 Bremerhaven, Germany.

planktic foraminifers, little knowledge exists of small scale events in time and space within the population of planktic foraminiferal species.

SPINDLER *et al.* (1979) were the first to document that reproduction in the planktic foraminifer *Hastigerina pelagica* (d'Orbigny) is coupled to the synodic lunar cycle. ALMOGI-LABIN (1984) has shown that *G. sacculifer* reproduces with full moon in the Gulf of Elat/Aqaba. Based on a time series of plankton-net tows, a synodic lunar reproductive cycle in *G. sacculifer* has been demonstrated by BIJMA *et al.* (1990) and subsequently confirmed by EREZ *et al.* (1991). Samples collected during scientific cruises into the Red Sea, the northeast Atlantic Ocean, and many blue water SCUBA dives in the Caribbean Sea also document the concept of lunar cyclicity in the life cycle of this and other planktic species (unpublished results).

Time, however, is only one factor in the life cycle of planktic foraminifers. Their depth migration during ontogeny is the second factor that determines the population dynamics of a species. SCHMIDT (1984) suggested, on the basis of stratified plankton tows, the life cycle of most tropical spinose foraminifera is dependent on the lunar cycle and that they descend to a deeper habitat during ontogeny. In this paper we discuss the depth and time components of the population dynamics of *G. sacculifer* from the central Red Sea in order to provide a better basis for paleontological interpretation. It will be demonstrated that this model species does not inhabit a specific depth, but migrates up and down in the water column during its ontogeny. The depth range is probably dependent on the hydrological conditions and may thus differ for different water masses.

2. MATERIALS AND METHODS

2.1. *Plankton samples*

During the RV *Meteor* cruise five, legs two and five (1987), stratified plankton samples were collected in the Red Sea (Table 1; Fig. 1). A multiple open and closing net (MN) with a 0.5 × 0.5 m mouth opening, equipped with five nets of 100 μm mesh size, was employed for vertical tows. The upper 500 m of the water column were sampled at standard depth intervals: 0–20, 20–40, 40–60, 60–80, 80–100, 100–200, 200–500 m. Most samples were taken in the central Red Sea, but some were taken in the southern part (Table 2B, Fig. 1). During leg two (February–March) the northeast-monsoon prevailed, and during leg five (July–August) the southwest-monsoon was at its height. In terms of a lunar timescale, the samples are more or less evenly distributed over 1 lunar month (Table 2A).

The samples were fixed in 2–4% hexamethylene-tetramine buffered formalin and processed in our laboratory in Tübingen. To separate the mineralized plankton (foraminifers, radiolarians, ostracods, heteropods, pteropods), the samples were washed with tap water over a column of sieves. Each sieve fraction and its water residue was poured into a petri dish which was rotated to concentrate the organisms with hard parts in the center. The skeletons were pipetted off and dried at room temperature. From these samples, all *G. sacculifer* were picked and the maximum diameter was measured, first under the binocular and at a later stage with an image analysis system [image processor board VS-100-AT of Imaging Technology; Sony CCD camera (AVC-D5CE) with a resolution of 760 × 512 pixels; Optima software (1989)]. Size measurements with both methods gave comparable results. Nine size classes of 100 μm width were formed (BIJMA *et al.*, 1993). Because the plankton net mesh was 100 μm, the size classes start at 100 μm as well.

Table 1. *Location of the stations, date and time of collection of each multinet (MN) and the numbers per cubic meter (no.* m^{-3}*) of* G. sacculifer *collected. The depth of the thermocline, temperature and density at* 80 m *depth are taken from* VERCH et al. (1989*a*;*b*). *The depths of the chlorophyll maxima are from* WEIKERT et al. (1988)

MN	Station	Latitude (°N)	Longitude (°E)	Date	Time	Lunar day	Depth-range (m)	Thermocline (m)	Density (80 m)	Temperature (80 m)	Chlorophyll maximum	No. m^{-3}
7	108	21.26	38.01	02/12	12.40	28	100–200–500	20	27.754	23.27	—	1.7
8	108	21.26	38.01	02/12	14.00	28	0–20–40–60; 80–100	20	27.754	23.27	—	2.7
9	116	21.26	37.54	02/13	18.05	29	0—20–40–60–80–100	—	—	—	—	3.3
15	132	21.21	38.05	02/16	17.50	3	100–200–500	12	27.756	23.22	—	0.3
16	137	20.02	38.26	02/18	10.50	5	100–200	100	26.204	25.95	—	1.1
20	181	19.09	39.07	02/25	15.40	12	100–200–500	—	—	—	—	0.6
37	269	13.11	47.05	03/13	14.10	28	0–20–40–60–80–100	no	24.596	23.43	—	2.6
39	272	13.21	47.31	03/14	07.10	29	0–20–40–60–80–100	100	—	—	—	4.2
54	627	11.56	43.43	07/10	19.20	28	0–20–40–60–80–100	20	—	—	—	1.3
63	642	18.42	39.21	07/14	15.55	3	0–20–40–60–80–100	—	—	—	70	15.4
64	643	22.26	36.60	07/15	20.15	4	0–20–40–60–80–100	25	27.514	23.93	80	16.8
65	643	22.26	36.60	07/15	20.50	4	100–200–500	25	27.514	23.93	80	0.0
66	646	22.57	37.01	07/16	05.30	5	0–20–40–60–100	30	26.830	24.84	—	8.2
67	646	22.57	37.01	07/16	06.05	5	100–200–500	30	26.830	24.84	—	0.1
68	653	23.24	36.13	07/17	06.05	6	0–20–40–60–80–100	20	27.904	22.95	—	1
69	653	23.24	36.13	07/17	06.40	6	100–200–500	20	27.904	22.95	—	0.1
72	660	23.39	36.37	07/18	20.50	7	0–20–40–60–80–100	40	27.497	23.90	—	13.7
74	662	23.06	37.14	07/20	04.25	9	0–20–40–60–80–100	30	27.003	25.04	—	27.0
75	662	23.06	37.14	07/20	05.00	9	100–200–500	30	27.003	25.04	—	0.2
78	674	19.40	38.41	07/22	22.55	11	0–20–40–60–80–100	30	26.538	25.45	—	7.9
79	674	19.40	38.41	07/22	22.25	11	100–200–500	30	26.538	25.45	—	0.1
83	679	20.58	38.10	07/24	17.55	13	0–20–40–60–80–100	—	—	—	—	13.7
84	679	20.58	38.10	07/24	18.25	13	100–200–500	—	—	—	—	0.1
86	682	21.14	38.05	07/25	21.10	14	100–200–500	—	—	—	—	0.3
89	691	21.27	37.59	07/27	15.00	16	0–20–40–60–80–100	—	—	—	80	20.2
90	692	21.19	38.06	07/27	19.50	16	100–200–500	—	—	—	—	0.1
91	695	19.40	38.42	07/29	03.50	18	0–20–40–60–80–100	—	—	—	80	3.0
92	695	19.40	38.42	07/29	04.25	18	100–200–500	—	—	—	80	0.2
94	701	19.02	39.08	07/30	19.05	19	0–20–40–60–80–100	—	—	—	—	4.8
96	702	15.52	41.44	08/03	05.10	23	0–20–40–60–80–100	40	26.595	24.96	30	0.5
97	702	15.52	41.44	08/03	05.40	23	100–200–500	40	26.595	24.96	30	0.1
98	704	15.14	41.55	08/04	01.50	24	0–20–40–60–80–100	25	27.094	24.29	40	0.5
104	710	12.60	43.11	08/06	02.15	26	0–20–40–60–80–100	25	26.064	18.48	—	1.0
Multicorer												
97	146	19.45	37.38	02/19			600 m					

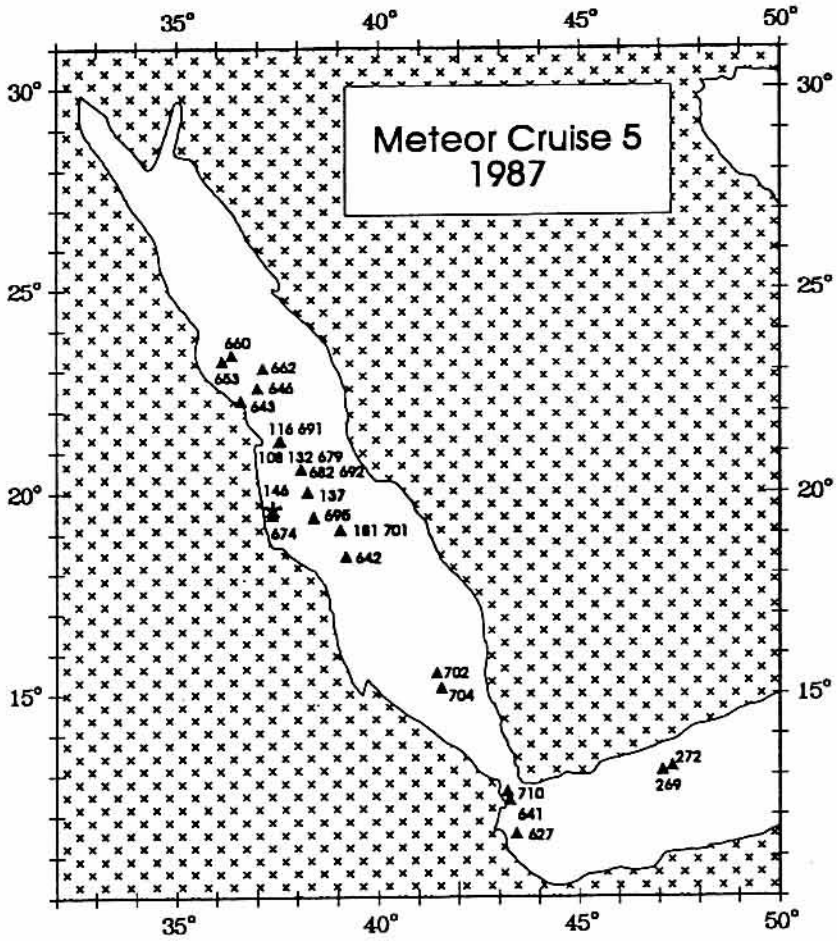

Fig. 1. Sampling stations; triangles are multinet stations and an asterisk indicates the location of multicorer sediment sample.

According to BRUMMER *et al.* (1987) the neanic stage for *G. sacculifer* starts between 75 and 100 μm. Thus, in terms of ontogeny, our data are quantitative from the late neanic stage onwards. Absolute numbers per cubic meter were calculated by dividing the total number by the filtered water volume (i.e. MN mouth area × depth interval).

2.2. *Calculation of residual values*

To evaluate the population structure of *G. sacculifer* as a function of depth and time, 4300 specimens were picked and measured. To establish the depth habitat where growth takes place, changes in the population structure with depth were analysed. After determination of the reproductive depth, the change in depth habitat during ontogeny was studied. The water column above the reproductive depth is defined as the productive zone. Once the productive zone was determined, the population changes within this zone as a function of time were investigated.

To evaluate changes in the depth distribution, the data for all stations (except the incomplete MN 8 and MN 66; Table 1) were combined, independent of their collection time. First, the mean absolute number of *G. sacculifer* in nine size fractions was calculated for each depth interval and for each depth interval, the relative frequency and the mean of

Table 2. Selected multinet samples (MN) and the average number of specimens per cubic meter in the upper 80 m *of the water column* (n). (A) *Data are arranged according to lunar day (time of collection) and,* (B) *according to latitude respectively*

(A)				(B)		
MN	Day	Time	*n*	MN	Latitude	*n*
63	03	15:55	19.2	98	15,14	0.6
64	04	20:15	20.3	96	15,52	0.6
68	06	06:05	1.3	63	18,42	19.2
72	07	20:15	15.9	94	19,02	5.8
74	09	04:25	32.1	78	19,40	9.0
78	11	22:55	9.0	91	19,40	3.6
83	13	17:55	16.2	83	20,58	16.2
89	16	15:00	24.5	89	21,27	24.5
91	18	03:50	3.6	64	22,26	20.3
94	19	19:05	5.8	74	23,06	32.1
96	23	05:10	0.6	68	23,24	1.3
98	24	01:50	0.6	72	23,39	15.9
37	28	04:10	3.1			
39	29	07:10	4.6			

G. sacculifer within each size class was determined. In the last step, the residual values were calculated by subtracting the mean relative frequency of a size class from the actual relative frequency of that size class for each depth interval. The result of this procedure is a size/depth matrix with positive and negative numbers. Using a contour program the zero isoline, separating negative from the positive areas, was plotted. The positive areas in the contour plot indicate depth-habitat preferences of each size fraction. The advantage of this procedure is that the signal of the coarser size fractions, which are less abundant, is not lost (see also Bijma *et al.*, 1990).

In order to evaluate changes in the population structure versus time, the data for the productive zone (upper 80 m) were combined for each station. Because seasonality may bias the results, the data-set was restricted to one season. Because most samples were taken during the southwest monsoon, samples taken during the northeast monsoon (MN 9, MN 37; MN 39) were not incorporated in the analysis.

Since the reproduction cycle of *G. sacculifer* shows a monthly recurring pattern, the samples were sorted according to their collection time within the lunar cycle. Residual values were calculated for nine size classes collected on 15 different days in the lunar cycle. Contour plots were generated for the productive zone as a whole and for each 20 m depth interval separately. The best results were obtained for the interval 40–60 m. To reduce the noise in the graph, the first contour was not started at 0, but at 0.15. In other words, the contour plot shows maximum occurrences of certain size classes with respect to the lunar cycle.

2.3. *Mortality and survival*

Shells sink to the ocean floor after death or reproduction. After death, the shells contain pale cytoplasm while sinking, while after reproduction the settling "mothershell" is empty.

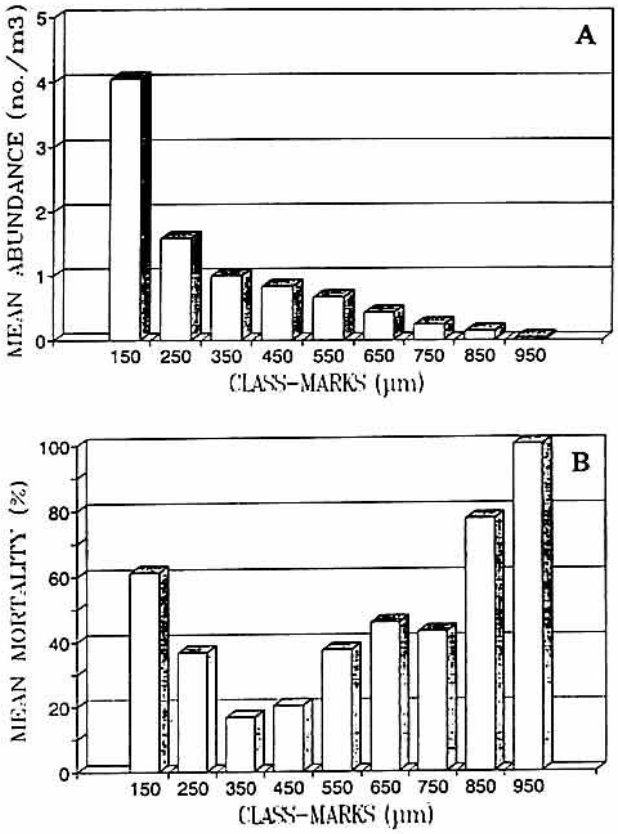

Fig. 2. (A) Mean abundance (no. m^{-3}) of *G. sacculifer* >100 μm in the upper 80 m of the central Red Sea. All stations except Stations 108 and 646 were used. The class-marks are plotted on the *x*-axis. (B) Mean mortality during one life cycle for each size class. For explanation see text.

To determine the loss rate of each size fraction within the productive zone, a mortality curve was generated (Fig. 2). Hereto, the mean number of specimens within the upper 80 m, collected during 1 lunar month, was calculated for each size fraction (the incomplete stations MN 8 and MN 66 were not used for this purpose; Table 1; Fig. 2A).

The difference between one size class and the next is equivalent to the mortality in the former size class (Fig. 2B). From the assemblage that settles to the ocean floor, most have died before reproduction and the mortality decreases towards the size fraction 300–400 μm but increases from this size class to larger fractions, presumably as a result of reproduction.

To estimate the frequency of gametogenesis in each size fraction, the last chamber morphology was inspected. Laboratory cultures have demonstrated that the formation of a sac-like or a diminutive chamber precedes gamete release by 24–48 hours (HEMLEBEN *et al.*, 1987). Thus, the presence of kummerform and sac-like chambers indicates that specimens have undergone gametogenesis (HEMLEBEN *et al.*, 1989). Normalform specimens conserve traces of gametogenesis in the ultrastructure of the shell. Non-gametogenic adult specimens have sharp interpore ridges made up of stacked calcite plaques. These terraced structures are organized in a well-developed polygonal pattern, the so called cancellate surface texture. In gametogenic specimens, spines have been actively resorbed, leaving behind spine-holes, the sharp interpore ridges have developed into broad interpore areas due to a smooth veneer of calcite known as gametogenic (GAM) calcification.

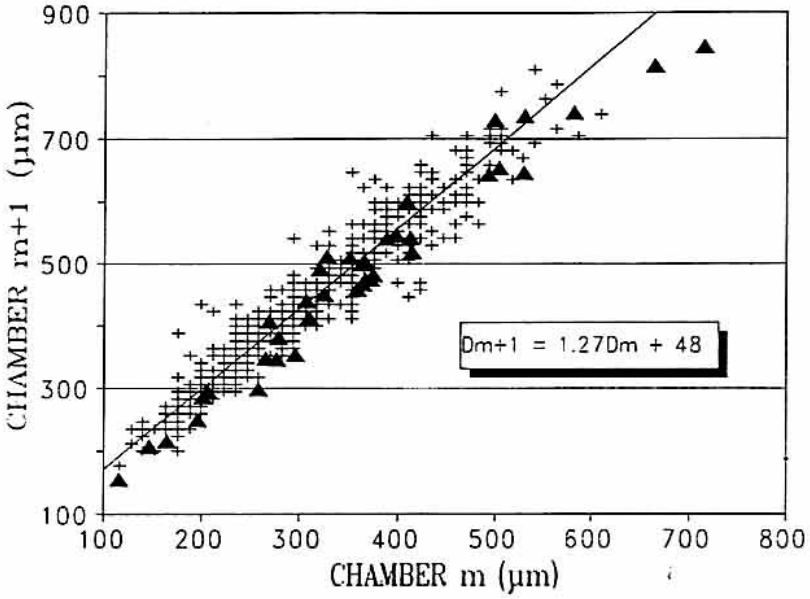

Fig. 3. Growth curve of *G. sacculifer* from laboratory cultures (+); for comparison, data from TAKAHASHI and BÉ (1984) are also shown (filled triangle). The solid line is the least squared fit to our data points and is described by $D_{m+1} = 1.27D_m + 48$, where D_m and D_{m+1} are the m^{th} and $m + 1^{th}$ chamber, respectively.

In more advanced stages of GAM-calcification, the spine-holes may become covered with calcite and thus difficult to detect (BÉ, 1980; HEMLEBEN *et al.*, 1989, 1991). Thus, the frequency of gametogenesis within each size class can be estimated by adding the fractions or irregular morphotypes and post gametogenic normalform shells. Here, we inspected 189 normalform specimens from several samples between 100 and 500 m depth, with a SEM.

2.4. *Sediment sample*

A representative sediment surface sample (0–0.5 cm) was recovered by means of a multicorer (MC97) from the central Red Sea (19°45, 5'N,37°38,4'E; 600 m depth; Fig. 1). The sample was split into five sieve fractions (<250, 250–315, 315–400, 400–500 and >500 µm). To compare the sediment with the plankton, the sieve sizes must be converted to absolute size. The gross shell morphology of normalform *G. sacculifer* allows a simple conversion of sieve size into real shell size; the sieve size of a specimen corresponds to the real maximum diameter of the previous stage of growth of the same specimen. The conversion may thus be read directly from a growth curve (Fig. 3) and this growth curve is based on laboratory cultures of *G. sacculifer* grown at the Bellairs Research Institute, Barbados, during the years 1980–1984 (HEMLEBEN *et al.*, 1987). Only specimens that had undergone gametogenesis were used for the growth curve. In total 206 specimens were used that had formed 519 chambers altogether. On basis of the growth curve, the real size intervals of the sediment fractions are as follows: <366, 366–448, 448–556, 556–683 and >683 µm.

The morphotype distribution within each of these fractions was determined by counting the whole subsample or at least 300 specimens. In each fraction the percentage of gametogenic specimens was determined by SEM inspection at a magnification of 1000×;

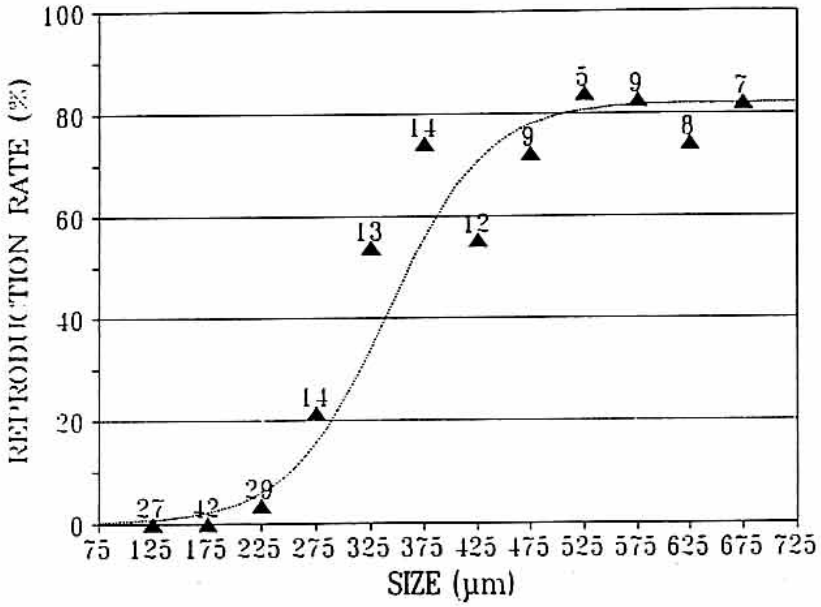

Fig. 4. The reproduction rate of *G. sacculifer* as a function of size is calculated as the sum of the percentage of normalform specimens with GAM-calcification plus the percentage of SAC, KUM and KUMSAC specimens in each size fraction. The numbers of normalform specimens that were investigated with the SEM in each size fraction are given above each data point. The first and the last size fractions are <150 and >650 μm, respectively. The other size fractions are equidistant and 50 μm wide.

20 normalform specimens were picked at random from each fraction (the fraction <366 μm contained only 15 specimens).

3. RESULTS

Each sample represents a transient state of the standing stock and is effected by the time of collection (daytime, lunar day, season), depth and latitude. Although the clustering of all samples over time and space need not represent the dynamics of one single population, we assume that it does so as long as the scales of time and space are small enough. Although, the density of *G. sacculifer* is dependent on latitude (AURAS-SCHUDNAGIES *et al.*, 1989), we assume that a similar depth distribution occurs and that the development is comparable between all stations.

3.1. *Maturation*

The relationship between reproduction and size can be described by a sigmoidal curve (Fig. 4);

$$\text{reproduction rate (\%)} = \frac{82}{1 + e^{(7.5 - 0.022 \times \text{size})}}.$$

Gametogenesis is unusual below 250 μm, the frequency increases exponentially between 300 and 400 μm and reaches a maximum of 82% after a size of approximately 500 μm. At 366 μm, a reproduction rate of more than 50% is reached. For first approximation, we use 366 μm (250 μm sieve size) as the size at which maturation occurs. This is in agreement with the shape of the mortality curve. Apparently, the increasing loss rates after maturation are due to reproduction (Fig. 2B).

Table 3. Estimated percentage of gametogenic specimens in a representative core top sample from the central Red Sea (MC 97) *is given in five size fractions; No. = number of specimens in aliquot;* n = *absolute numbers; per cent = relative frequency for each of the morphotypes (SAC = sac-like, KUM = kummerform, KUMSAC = diminutive sac-like, NOR = normalform); GAM = relative frequency of gametogenetic calcification in normalform specimens; total = frequency of gametogenesis in each size interval*

Sieve fraction (μm)	Size interval (μm)	No.	SAC		KUM		KUMSAC		NOR		GAM	TOTAL
			(*n*)	(per cent)	(*n*)	(per cent)	(*n*)	(per cent)	(*n*)	(per cent)	(per cent)	(per cent)
<250	<366	15	0	0	0	0	0	0	15	100	100	100
250–315	366–448	237	48	20	6	3	0	0	183	77	100	100
315–400	448–556	336	81	24	36	11	7	2	212	63	100	100
400–500	556–683	360	142	39	24	7	13	4	181	50	100	100
>500	>683	357	152	43	43	12	25	7	137	38	100	100
	Total	1305	423	32	109	8	45	4	728	56	100	100

In sharp contrast to the settling assemblage do all sediment specimens show signs of gametogenesis (Table 3).

3.2. *Bathymetric distribution*

The number of *G. sacculifer* shells decreases drastically with depth. On the basis of numbers per m^3, 95% of the shells collected in the upper 500 m of the water column live in the upper 80 m (Fig. 5). not only the absolute abundance changes with depth, the size distribution is also different for each depth interval (Fig. 6A–G). The small fraction (<300 μm) dominates the water column but their relative frequency decreases with depth until, between 60 and 80 m depth, the larger fractions (>300 μm) become dominant. Below 80 m depth, however, the small size fraction starts to dominate again. A cumulative plot of the

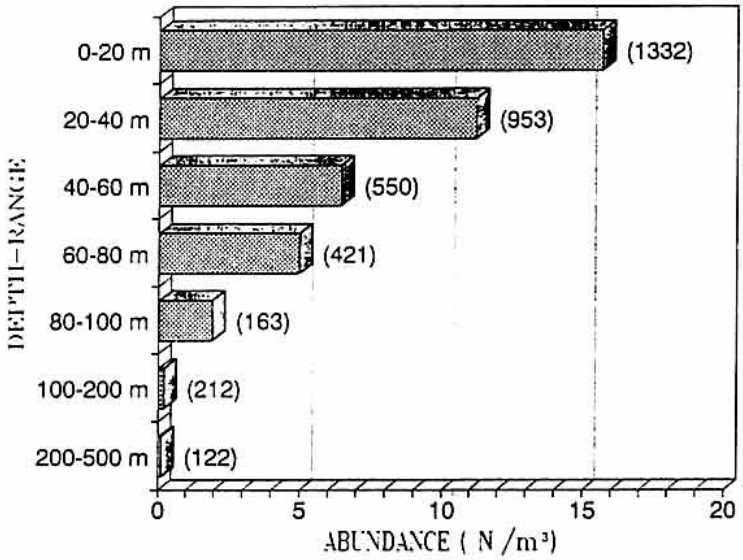

Fig. 5. The mean abundance (no. m^{-3}) of *G. sacculifer* (>100 μm; collected in the period 12 February–6 August in the central Red Sea) decrease with increasing depth. The total numbers are given in parentheses.

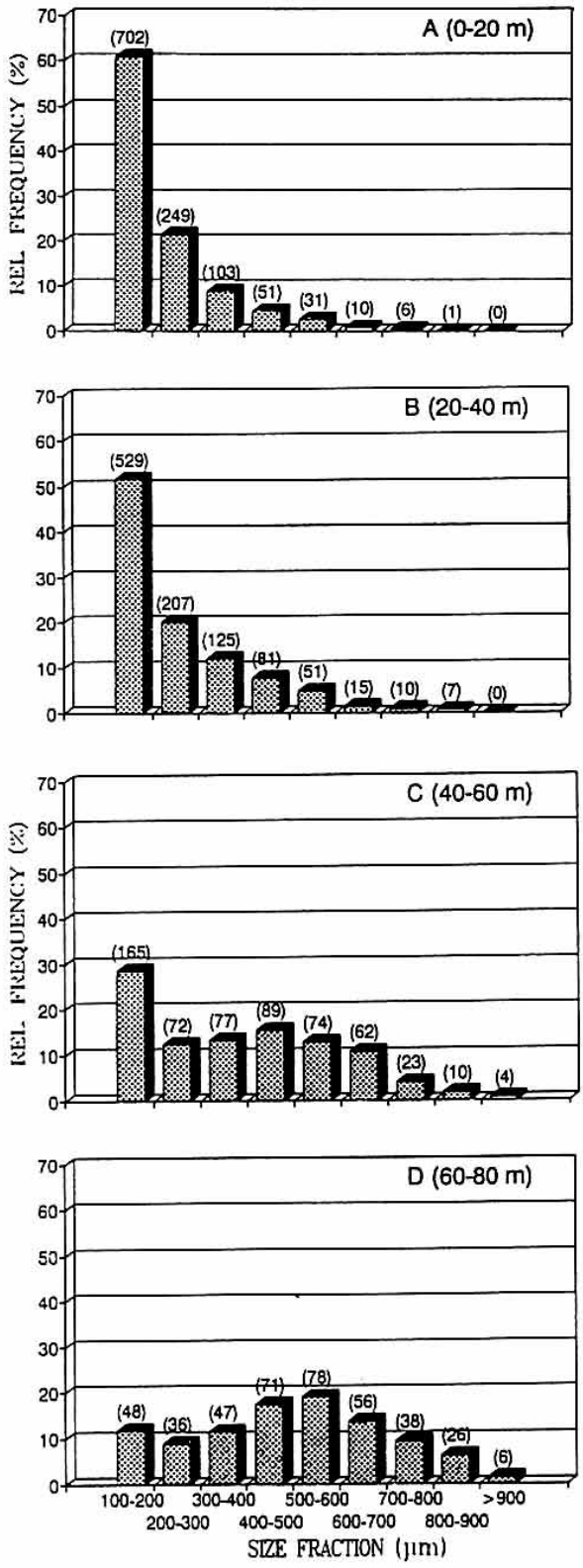
A (0-20 m)
(702)
(249)
(103)
(51)
(31)
(10)
(6)
(1)
(0)
B (20-40 m)
(529)
(207)
(125)
(81)
(51)
(15)
(10)
(7)
(0)
C (40-60 m)
(165)
(72)
(77)
(89)
(74)
(62)
(23)
(10)
(4)
D (60-80 m)
(48)
(36)
(47)
(71)
(78)
(56)
(38)
(26)
(6)
REL. FREQUENCY (%)
0
10
20
30
40
50
60
70
100-200
200-300
300-400
400-500
500-600
600-700
700-800
800-900
>900
SIZE FRACTION (µm)

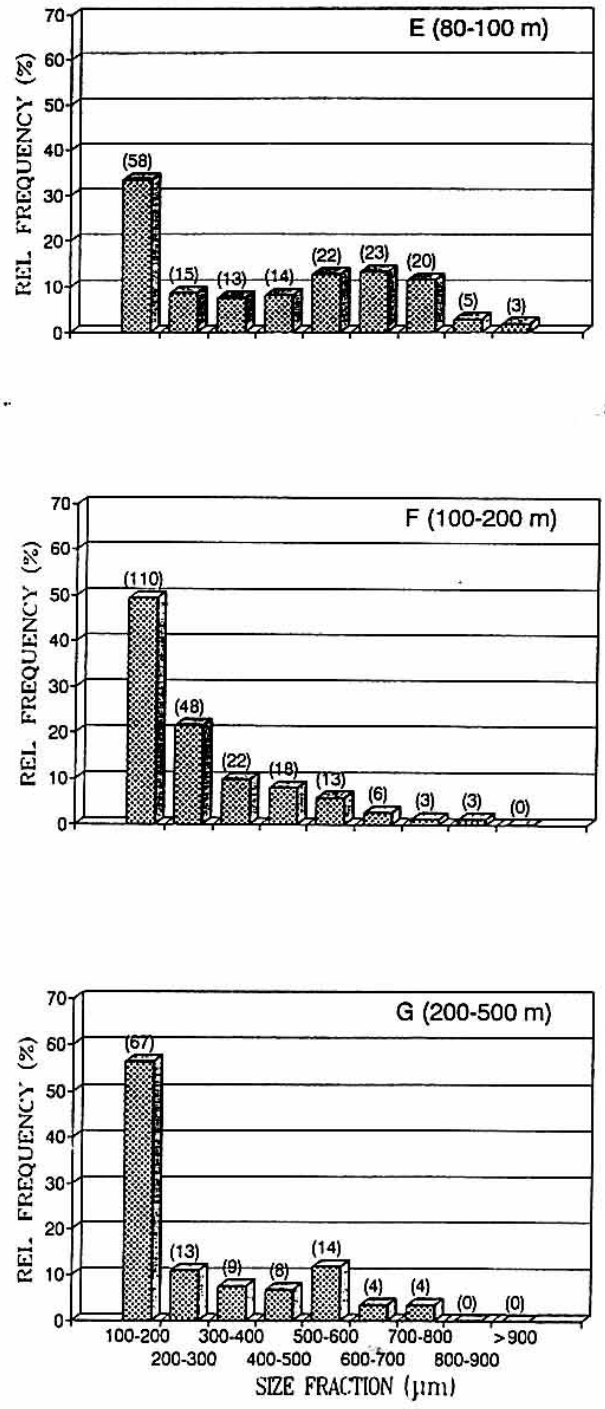

Fig. 6. The relative frequency of nine equidistant size classes as a function of depth (A) 0–20 m, (B) 20–40 m, (C) 40–60 m, (D) 60–80 m, (E) 80–100 m, (F) 100–200 m, and (G) 200–500 m. All stations (12 February–6 August) were used and specimens were measured individually (the total numbers are given in parentheses).

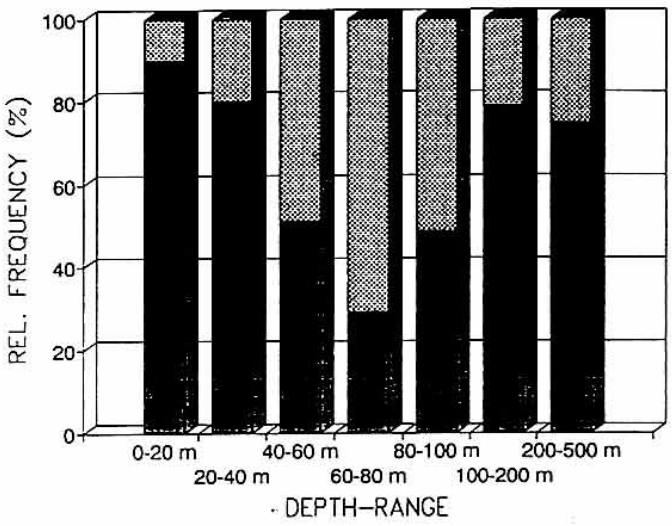

Fig. 7. The frequency (%) of mature (>366 μm; shaded) and immature (<366 μm; solid black) *G. sacculifer* show a characteristic break between 60 and 80 m depth (based on Fig. 5).

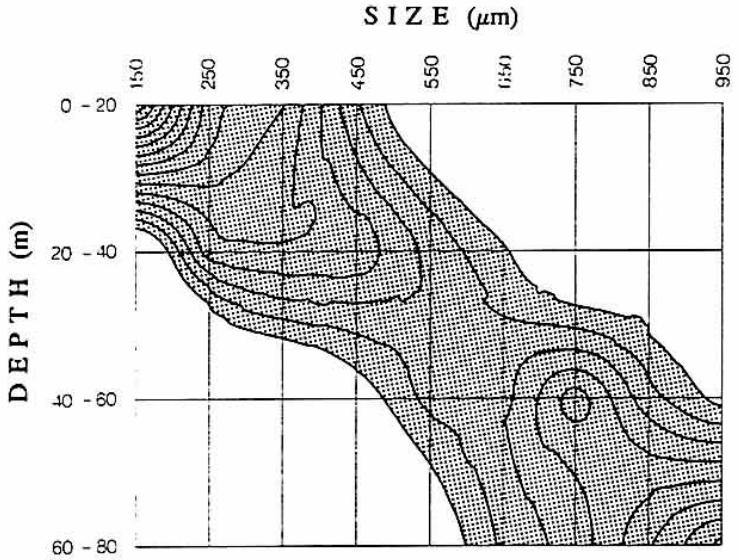

Fig. 8. Contour plot of residual values in a size–depth frame, showing that larger size fractions prefer deeper depth-habitats. The calculation of the residuals is based on all stations (12 February–6 August) where the upper 80 m was sampled in 20 m intervals (except 108 and 646). The cross-sections of the grid represent the data points. The centers of the nine size fractions (100 μm wide) and the depth intervals are listed. The shaded area contains positive residual values, indicating a larger than average presence of a size fraction. The isolines start with 0 and are drawn at 0.05 intervals. The blank area contains negative residual values, indicating a smaller than average presence of a size fraction.

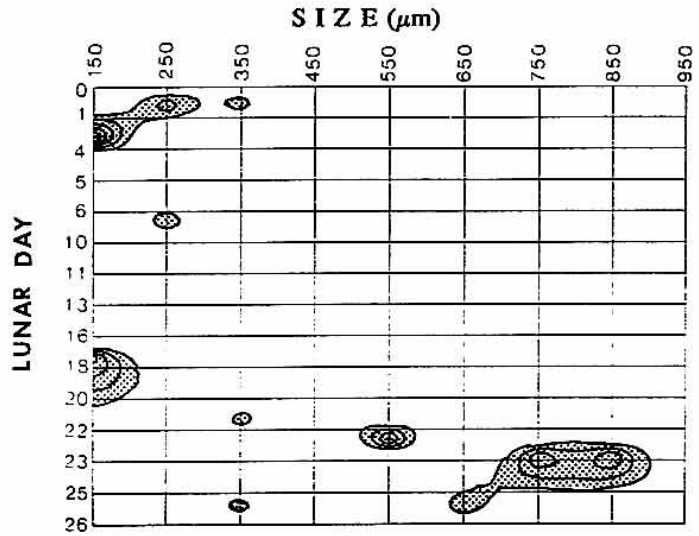

Fig. 9. Contour plot of residual values (between 40 and 60 m depth) in a size–time frame. The calculation of the residuals is based on samples that were collected between 12 February–6 August. The cross-sections of the grid represent the data points. The centers of the nine size fractions (100 μm wide) and 15 days in the lunar cycle are listed (full moon at 0 and 29). The shaded areas contain residual values larger than 0.15, and isolines drawn at 0.05 intervals. The blank area contains residual values smaller than 0.15. For explanation see text.

relative frequency of mature (>366 μm) and immature specimens (<366 μm) versus water depth demonstrates a bimodal pattern with a breakpoint between 60 and 80 m depth (Fig. 7). The maximum of mature specimens coincides with the depth range 60–80 m. The relative number of immature specimens increases towards shallower and deeper environments (Fig. 7). Accordingly, on the basis of vertical plankton tows, three zones can be distinguished in the water column: (1) a productive zone, where growth takes place; (2) a small intermediate zone where reproduction takes place; and (3) a flux zone with post-gametogenetic (empty) and dead shells (empty or filled with various amounts of cytoplasm) on their way to the ocean floor. Dead or dying specimens may be recognized by the pale color of their cytoplasm. In contrast, the cytoplasm of living specimens is yellowish to brownish, or greenish (depending on the symbionts, food vacuoles), and turns reddish prior to reproduction due to lipid production.

The life cycle of *G. sacculifer* is restricted to the productive zone. The contour plot demonstrates size-dependent depth preferences (Fig. 8). In three dimensions, the plot has the shape of a saddle, where the heights indicate maximum abundance. The plot thus demonstrates that the upper 20 m are the preferred habitat for immature specimens between 100 and 300 μm. The depth range between 20 and 40 m is favored by specimens from 300 to 500 μm. This is the depth where maturation takes place. Specimens between 500 and 700 μm prefer a depth range between 40 and 60 m, and specimens larger than 700 μm are found at the reproduction depth between 60 and 80 m water depth (Fig. 8).

3.3. *Time distribution*

The contour plot of the depth interval of 40–60 m shows that the population develops from predominantly immature specimens just after full moon to a maximum of terminal specimens just before full moon (Fig. 9). Contour plots also were generated for the

Table 4. (A) *Total numbers and percentages of morphotypes calculated from all samples. NOR = normalform, SAC = sac-like chamber s.s., KUM = kummerform, KUMSAC = intermediate form between KUM and SAC. The average maximum test diameter, the median, minimum and largest maximum test diameter for each of these morphotypes are listed (lower size is 100 μm). In addition to the samples listed in Table 1 we used other samples collected during the same cruise. For explanation see text.* (B) *Plus indicates significantly different pairs on the basis of a 95% Scheffé test of maximum test diameter*

(A)	NOR	KUM	KUMSAC	SAC
n	4033	23	62	164
Per cent	94	1	1	4
Average (μm)	264	300	627	711
Median (μm)	200	206	650	725
Minimum (μm)	59	106	175	300
Maximum (μm)	950	750	875	1050

(B)	NOR	KUM	KUMSAC	SAC
NOR	–	–	+	+
KUM	–	–	+	+
KUMSAC	+	+	–	+
SAC	+	+	+	–

productive zone as a whole and for each of the other 20 m depth intervals separately. Apparently, the habitat preferences of certain ontogenetic stages influence the size–time contour plots.

3.4. *Distribution of morphotypes*

To date, three morphotypes have been recognized within *G. sacculifer* (HEMLEBEN *et al.*, 1987). The normalform final chamber (NOR) is equal in shape but larger in size than the previous one. Specimens with a diminutive last chamber, similar in shape to the previous chambers are referred to as kummerforms (KUM). The so-called sac-like morphotype is characterized by the sac-like shape of the ultimate chamber (SAC).

Here, a fourth type is distinguished, which intergrades between the kummerform and the sac-like morphotype (KUMSAC), i.e. a sac-like final chamber smaller than the penultimate one. With increasing size, the frequency of kummerform, sac-like and kummersac chambers increases relative to that of the normalform ones (Tables 3 and 4A). The mean maximum diameter and the median diameter of the intergrading kummersac morphotype is much closer to the mean size and the median diameter of the sac-like (senso stricto) than to the true kummerform morphotypes (Table 4A). A Scheffé test at 95% confidence level (WEBER, 1986) shows that the average final size of sac-like morphotypes and kummersacs are significantly different from each other (Table 4B). Both are significantly different from kummerform and normalform morphotypes. The size differences between kummerform and normalform are not significant. The frequency distribution of the four morphotypes was calculated as a function of depth (Fig. 10A–D) and as a function of lunar day (Fig. 11A–D). Because the total number of specimens decreases with depth (Fig. 5), the relative frequencies of the morphotypes between different depth

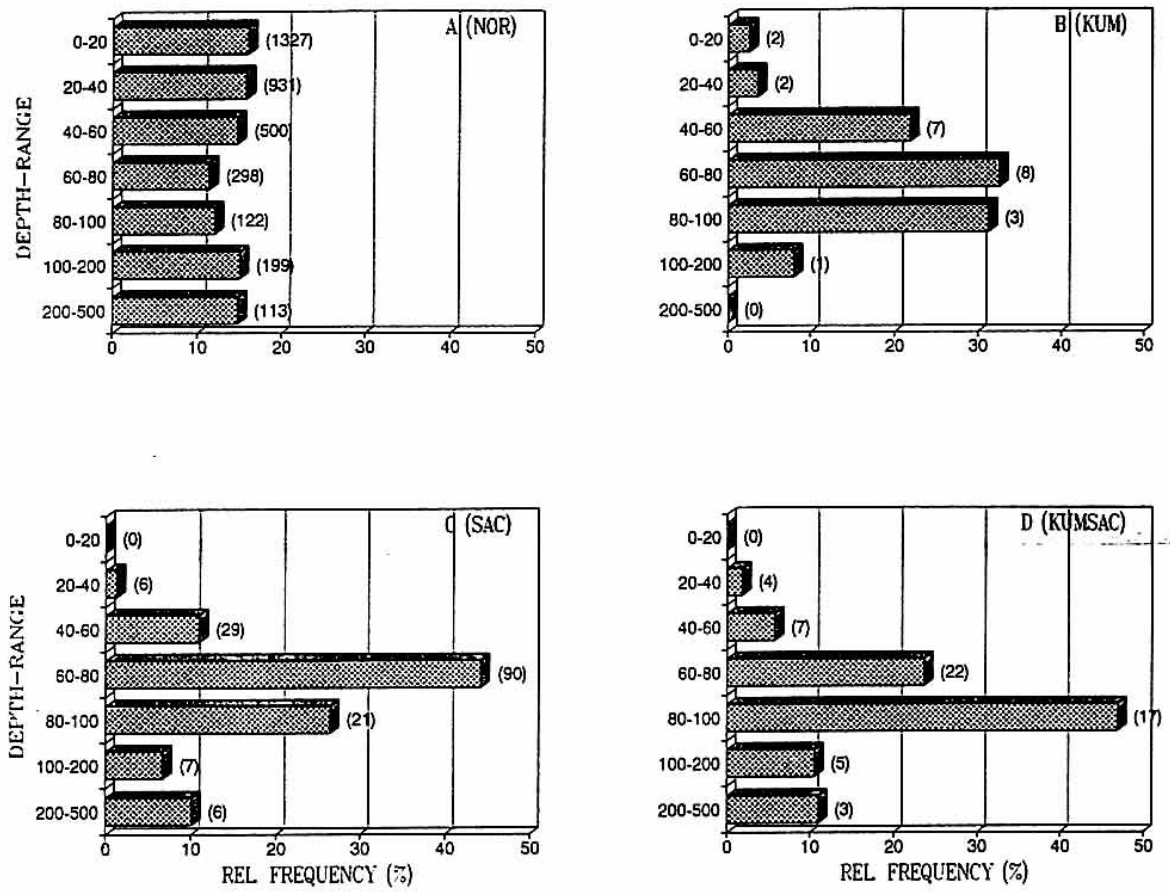

Fig. 10. The frequency distribution of each morphotype in the water column. The numbers are normalized to the total numbers collected in the upper 20 m of the water column (see text). (A) normalform; (B) kummerform; (C) sac-like; and (D) diminutive sac-like chambers. The total numbers are given in parentheses.

intervals cannot be compared directly. For instance, 29 sac-like morphotypes in a total catch of 550 specimens, between 40 and 60 m, is relatively less than 21 specimens in a total catch of 163 specimens between 80 and 100 m (Fig. 10C). To compensate for the difference in total catch per depth interval, the numbers must be normalized to the total catch in one depth interval (e.g. to the arbitrary chosen upper 20 m).

For comparison of morphotype frequencies between different time intervals, the numbers must be normalized as well because the total number of specimens was not equal for each time interval. Before calculating the relative frequencies, the numbers were normalized to the arbitrary chosen period of day 8–14.

Kummerform morphotypes are most frequent at intermediate depth (Fig. 10B) and just before full moon (Fig. 11B), concurrent with the depth and time of maximum distribution of mature specimens. Highest frequencies of sac-like specimens are found at the upper boundary of the reproductive depth (Fig. 10C) but contrary to kummerform chambers, they have a peak around new moon (Fig. 11C). Kummersac morphotypes are formed most frequently between 80 and 100 m water depth and like the kummerforms, usually before

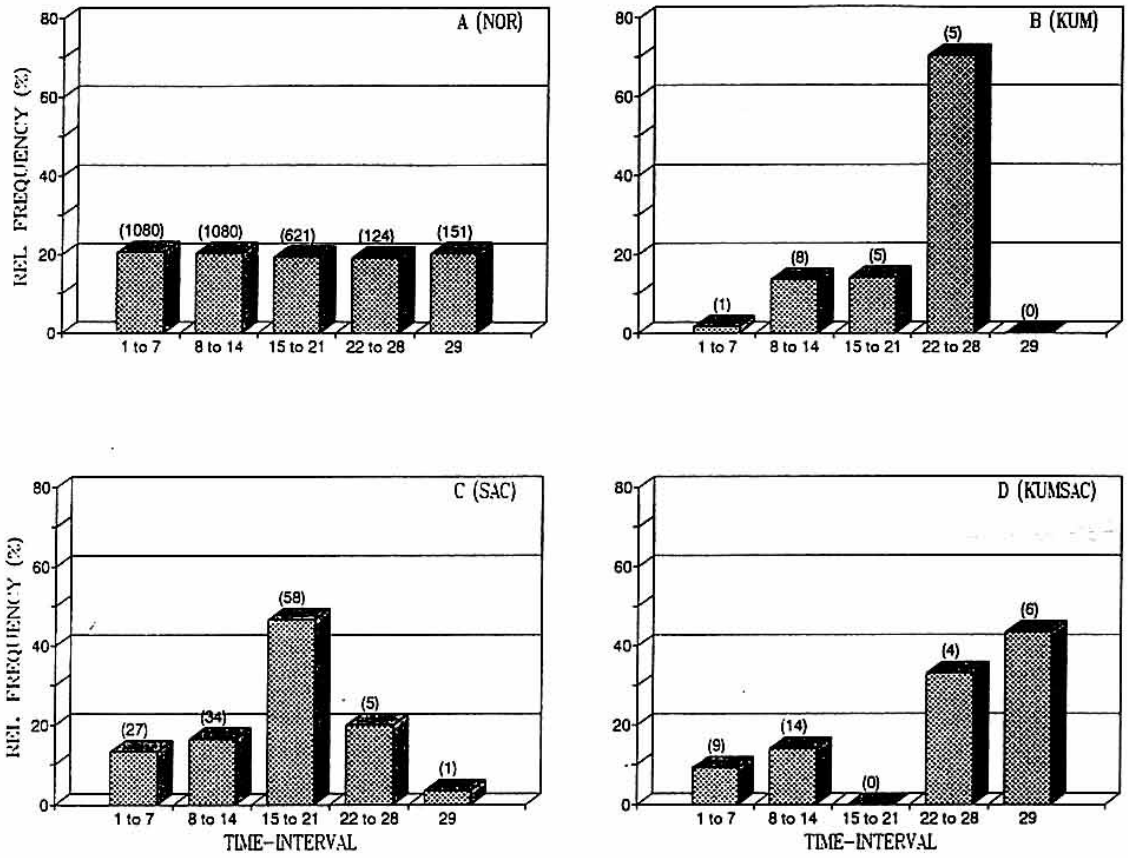

Fig. 11. The frequency distribution of each morphotype in the upper 80 m of the water column as a function of the lunar cycle. The numbers are normalized to the total number of specimens collected during the period 8–14 days in the lunar cycle (see text). 29 = Full moon. (A) normalform; (B) kummerform; (C) sac-like; and (D) diminutive sac-like chambers. The total numbers are given in parentheses.

full moon. The relative distribution of the four morphotypes as a function of depth and time is shown in Fig. 12A–B respectively.

3.5. *Flux and burial*

The flux assemblage and the sediment were analysed to compare the biocoenosis with the thanatocoenosis and to investigate any differences in population structure from the productive zone via the flux zone to the sediment surface.

Globigerinoides sacculifer shells below 80 m depth represent individuals settling to the ocean floor that have died or undergone gametogenesis. During settlement of *G. sacculifer* in the water column several parameters change. With the exception of the immature fraction (<366 μm), size (mean and median) increases through the production zone to the interval 80–100 m. From there downwards, the size of the mature fraction (>366 μm) generally decrease (Table 5A). In comparison to the settling *G. sacculifer* in the water column, the sediment is almost devoid of specimens <366 μm.

The relative proportions of normal, kummerform, sac-like or kummersac chambers do

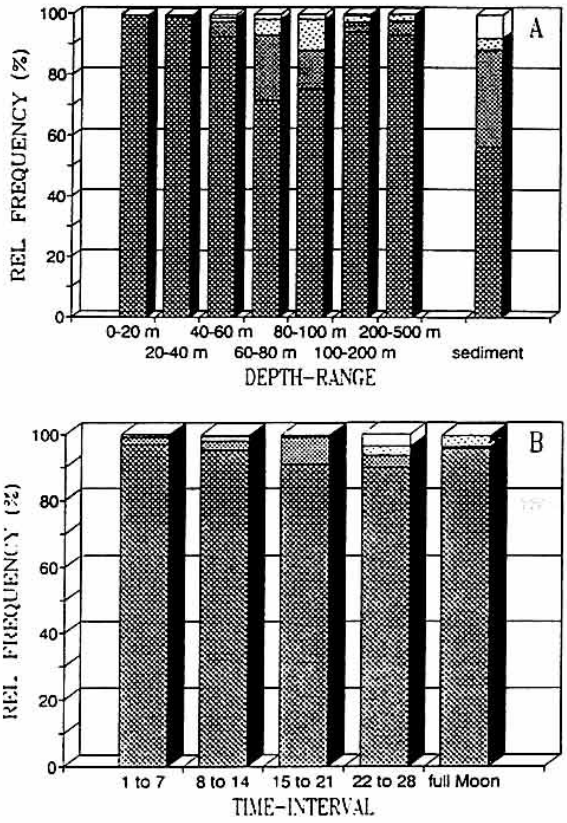

Fig. 12. The relative morphotype-distribution as a function of depth and in the sediment (A) and as a function of lunar day (B). Cross-hatched = NOR; dark shaded = SAC; light shaded = KUMSAC; and white = KUM.

neither change significantly with depth, nor for the population as a whole nor for the fraction <366 μm (Table 5B). We observed an increase of specimens with sac-like and kummersac chambers in the fraction 366–683 μm. The percentage of kummerform morphotypes does not change from depth-to-depth nor from fraction-to-fraction. In the fraction >683 μm, the numbers of observation are too low to show a distinct tendency. In comparison to the standing stock, the sediment is relatively depleted in normalform specimens (Table 5B, Figs 12A, 13A and B).

4. DISCUSSION

4.1. *Multiple regression analysis*

The mean abundance of *G. sacculifer* >100 μm in the upper 80 m of the water column is 9 specimens m^{-3}. However, the mean density decreases with increasing size (Fig. 2A). As *G. sacculifer* grows in the course of its life cycle, it is expected that the density in the productive zone decreases during the lunar month (Table 2A). Besides the lunar cycle, several other factors may influence the dynamics of a population as well. The samples were taken at different latitudes and at different times of the day (Tables 1 and 2). In addition,

Table 5. Changes in the population structure (specimens >100 μm) for three size classes and for the whole population in the water column (0–500 m); n = number of specimens. (A) Changes in mean size (s) and median size (m). (B) Changes in the relative distribution of the morphotypes

(A) Fraction	0–80 m			80–100 m			100–200 m			200–500 m		
	n	s	m	*n*	s	m	*n*	s	m	*n*	s	m
<366	2273	193	175	86	184	156	175	195	183	91	175	156
366–683	763	503	500	61	549	563	41	495	474	27	523	535
>683	160	781	763	30	791	775	7	774	806	4	761	769
Total	3196	296	225	177	414	390	223	269	202	122	271	175

(B)		0–100 m	100–200 m	200–500 m	Sediment
<366 μm	NOR	99	99	100	100
	SAC	0	0	0	0
	KUM	1	0	0	0
	KUMSAC	0	1	0	0
366–683 μm	NOR	90	81	74	62
	SAC	7	10	15	29
	KUM	0	2	0	7
	KUMSAC	3	7	11	2
>683 μm	NOR	41	28	50	38
	SAC	47	43	50	43
	KUM	2	0	0	12
	KUMSAC	10	29	0	7
Total	NOR	94	94	93	56
	SAC	4	3	5	32
	KUM	1	0	0	8
	KUMSAC	1	3	2	4

patchiness is an important component with regard to plankton distribution. Therefore, the possible effects of latitude and diel migration and patchiness shall be considered before the population structure of *G. sacculifer* is discussed in relation to depth and time.

The independent contributions of time and space to changes in standing stock can be estimated by statistical techniques. A multiple regression analysis of latitude, lunar day, day time, and number per cubic meter was carried out on a restricted data set. Only samples from the central Red Sea taken during the southwest monsoon were used (except MN 8 and MN 66)

$$n = 28.0 \times \text{latitude} - 6.8 \times \text{day} - 0.4 \times \text{time} - 63.6 \ (r^2 = 0.21).$$

The equation shows that the lunar day is not the most critical variable and that daytime contributes little to the variance in standing stock. The high standard error of the constant (± 733) shows that patchiness is an important component of the variance. The most critical variable seems to be latitude. However, because the samples at the end of the lunar cycle were taken progressively more south, the decrease in the course of the life cycle may be masked by a latitudinal effect.

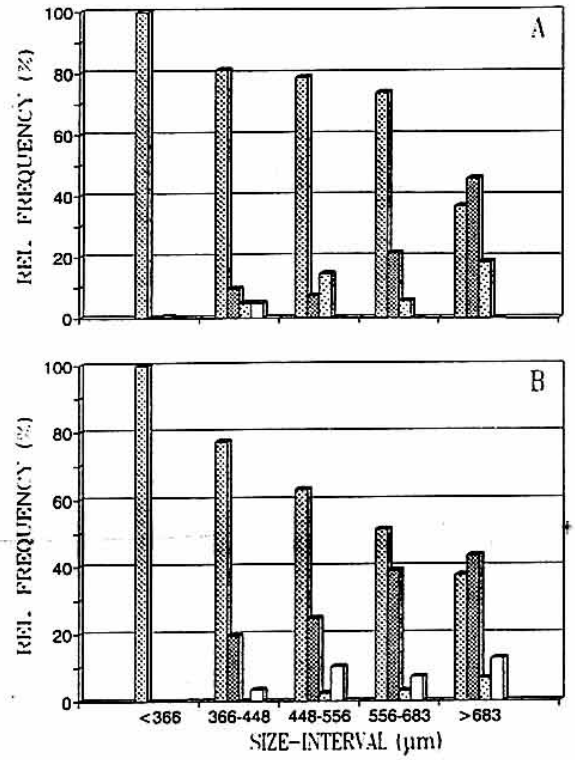

Fig. 13. The relative distribution of morphotypes in the upper 100 m (A) and in the sediment (B). Cross-hatched = NOR; dark shaded = SAC; light shaded = KUMSAC; and white = KUM.

4.2. *Latitude*

The decrease of *G. sacculifer* towards the south in the Red Sea (e.g. AURAS-SCHUDNAGIES *et al.*, 1989) has been suggested to be related to water fertility. Because the Red Sea loses water through evaporation, there is a continuous inflow of Gulf of Aden water into the Red Sea, supplying it with nutrient-enriched water. A north–south gradient is generated as the results of nutrient uptake as the water flows north (AURAL-SCHUDNAGIES *et al.*, 1989). The southwest monsoon causes strong upwelling off Oman and Somalia, which increases the nutrient gradient of the Red Sea intermediate water even more (GANSSEN and KROON, 1991). *Globigerinoides sacculifer* was found to be a low-fertility associated species (HALICZ and REISS, 1981). The dominance *G. sacculifer* in the oligotrophic Gulf of Elat/Aqaba (REISS *et al.*, 1980) also indicates its preference for low fertility environments. This explains why *G. sacculifer* becomes a less important component towards the south, where higher nutrient concentrations exist (Table 2A, Fig. 14A). However, parallel to the nutrients, the abundance of calanoid copepods also increases towards the south (WEIKERT *et al.*, 1988). It remains unexplained how nutrients restrict the abundance of *G. sacculifer* and why their numbers do not increase parallel with their food. Several other factors such as depth of chlorophyll maximum, thermocline etc. could be responsible (see, for example, WEIKERT, 1987).

The present investigation confirms that the density of *G. sacculifer* decreases towards the south (Table 2A, Fig. 14A). The mean number of *G. sacculifer* per cubic meter in the productive zone, however, also decreases in the course of the lunar month (Table 2B, Fig.

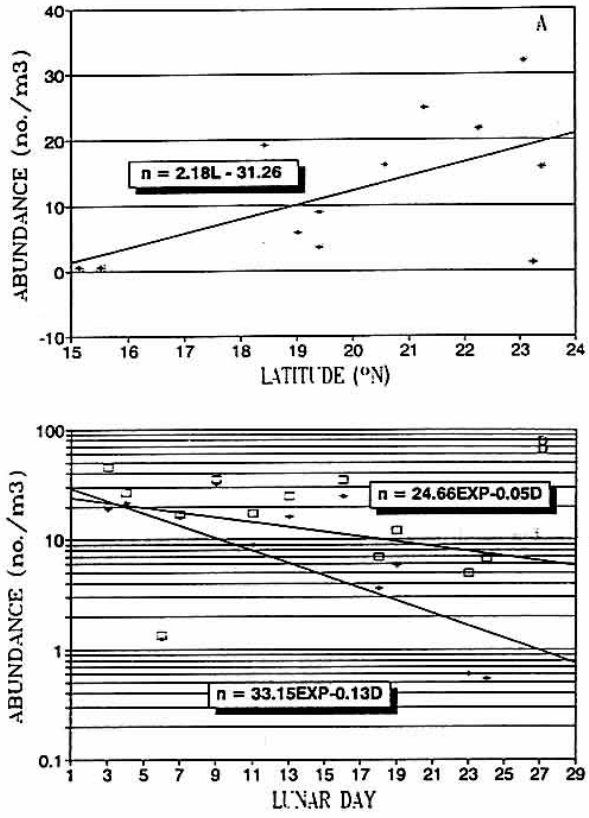

Fig. 14. Relationship between the average numbers per cubic meter of *G. sacculifer* >100 μm in the upper 80 m of the water column and (A) latitude (°N) and (B) the day of the lunar month. Only samples taken in the Red Sea during the southwest monsoon were used (asterisks). Open squares are values corrected for latitude. The numbers increase with latitude and decrease with the lunar day. For regression lines, regression relationships and the correction method see text.

14B). To estimate the decrease in standing stock in the productive zone due to the lunar cycle, a correction with respect to the latitudinal effect is applied. The samples from the Gulf of Aden (MN 54) and from the Strait of Bab el Mandeb (MN 104) were not incorporated in the calculations. The average number of specimens per cubic meter in the upper 80 m of the water column increases with latitude (Table 2A, Fig. 14A). The curve with the least sum of squares is $n = 2.18L - 31.26$ ($r^2 = 0.33$), where n is the average number of specimens per cubic meter in the upper 80 m and L is the latitude. We assume that the decrease during the life cycle follows a semi-logarithmic relationship ($N = N_o \times 10^{-at}$) because the survivorship can be approached by a log-linear function (Fig. 2A). Survival, however, cannot be linked directly to a definite time scale, and is therefore plotted as a function of size. Yet, we also assume a semi-logarithmic relationship with time because size increases as the life cycle progresses (Fig. 9). The regression line that fits the relationship best is $n = 33.15 \times 10^{-0.13D}$ ($r^2 = 0.39$), where n is the average number of specimens per meter cubed and D is the day in the lunar cycle. If the numbers per cubic meter are corrected for the decrease towards the south and normalized to 24°N, the regression relationship becomes: $N = 24.66 \times 10^{-0.05D}$ ($r^2 = 0.11$). Thus in comparison to the first, uncorrected, relationship, the decrease towards the end of the lunar cycle is reduced but still evident (Fig. 14B).

4.3. *Diel migration*

Multiple regression analysis showed that daytime contributes only insignificantly to the variance in standing stock. Some day and night samples from comparable stations and similar moments within the lunar cycle suggest that *G. sacculifer* descends to a deeper habitat at night (Table 2A; cf. MN 68 with MN 72, MN 78 with MN 83 and MN 91 with MN 94). However, in addition to the opposite migratory trend (Table 2A; cf. MN 37 with MN 39), samples from comparable times showed large differences (Table 2A; cf. MN 68 with MN 74). Consequently, the variation between day and night time samples can also be explained by patchiness and a diel migration pattern cannot be assumed for this species.

4.4. *Reproduction*

Analysis of *G. sacculifer* from 100 to 500 m depth in the water column shows that the reproduction rate increases exponentially in tests greater than 250 μm. At 366 μm, a reproduction rate of more than 50% is reached. This agrees with our laboratory observations that *G. sacculifer* normally reaches maturity at about 330 μm. The smallest specimen observed to produce gametes was 250 μm in diameter.

The mortality diagram (Fig. 2B) demonstrates that the loss rate in early ontogeny is very high but decreases with size before maturation. After maturation, reproduction is the main cause for the increased "mortality". Thus maturation takes place between 300 and 400 μm.

Around full moon, *G. sacculifer* releases hundreds of thousands of gametes. Only a fraction will fuse and develop into juveniles, and of these only a few will ascend to the surface layers of the water column (Fig. 6). Most specimens die and sink to the ocean floor as indicated by the increase of the fraction <366 μm below the reproductive depth (Fig. 7). Only a small fraction of the initial population will reach maturity and reproduce (Fig. 2).

Globigerinoides sacculifer descends to approximately 80 m depth in order to reproduce. The reproductive depth may be inferred from three phenomena. First, due to high mortality rates in early ontogeny there is a strong outfall of shells <366 μm (Fig. 2B). The increase of the immature size fraction below 80 m depth thus reflects dead specimens that sink to the ocean floor (Fig. 7). This observation sets the lower depth for reproduction to 80 m. Second, visual inspection of the samples immediately after collection revealed that the number of specimens with pale cytoplasm, reflecting dying or dead individuals increases drastically below 80 m depth. Third, the depth distributions of kummerform and sac-like morphotypes indicate that reproduction takes place somewhere between 60 and 100 m (Fig. 10B–D). We conclude that reproduction in the Red Sea during the monsoonal season takes place at about 80 m depth.

The reproductive depth is mostly below the thermocline, suggesting that the reproductive depth is not controlled by a strong temperature gradient nor by temperature itself. The temperature of the Red Sea at 80 m depth varied between 22.95 and 25.95°C (Table 1). A coincidence with a certain water density where gametes could concentrate also can be excluded. The mean density at 80 m depth is 26.88, but ranges from 24.6 to 27.9. The chlorophyll maximum zone is found from 30 m in the southern Red Sea to 80 m in the central Red Sea (WEIKERT *et al.*, 1988). Since most sampling was done in the latter region, a reproductive depth of 80 m would coincide with the depth of the chlorophyll maximum zone. This is also consistent with the observation of FAIRBANKS *et al.* (1982) that sac-like

chambers are associated with the chlorophyll maximum. The report that the reproduction depth of *G. sacculifer* in the Gulf of Elat/Aqaba is somewhere below 600 m (EREZ *et al.*, 1991) is based on the argument that lunar cycling could be demonstrated in tows from 200 to 600 m depth. However, because the authors did not differentiate between living and dead specimens we believe that the deep "population" represents dead and empty, post-gametogenic specimens. The cyclicity of the flux assemblage apparently reflects the dynamics of the living population.

It is important to realize that due to the mesh size of our collecting gear (100 μm), the data are not quantitative for specimens below 175 μm. Thus, the number of specimens in the size class 100–200 μm is biased towards lower numbers. Although the mesh size was 100 μm, specimens smaller than 100 μm were collected as well. The highest abundance of specimens <100 μm is found in the upper 20 m of the water column. We calculated that 76% of all specimens <100 μm were collected in the upper 20 m. Thus, juveniles have reached the surface before they become neanic (75–100 μm). By backtracking it can be calculated that specimens in this size fraction are already approximately 18 days old. Laboratory specimens of 220–250 μm require about 8–9 days to undergo gametogenesis (HEMLEBEN *et al.*, 1987). To grow from 100 to 220 μm, *G. sacculifer* requires another approximately 2–3 days. Thus, if the total life cycle is 29 days, it takes 17–19 days to reach 100 μm. The descending phase of the life cycle starts somewhere around 200 μm. They descend within 9–10 days to the reproduction depth and undergo gametogenesis.

4.5. *Morphologic response*

The distinction between the morphotypes is not always clear and intergrades between one type and the other, such as diminutive sac-like terminal chambers exist. Analysis with respect to size (Table 4) demonstrated that specimens with a diminutive sac-like chamber are closer related to the sac-like morphotype than to the normalform or kummerform morphotype. The mean maximum test size at the penultimate growth stage would be a better reference point for comparison because size would be unbiased by the shape of the last chamber. Using the maximum test size at the penultimate growth stage, the above relationships become even more explicit. It is therefore tempting to conclude that specimens with a diminutive sac-like chamber are formed by the same process as specimens with a sac-like chamber and that kummerform morphotypes are formed by the same mechanism as normalform specimens.

On the other hand, analysis with respect to time suggests that the kummerform and the kummersac morphotype are closely related. They are both formed predominantly around full moon. It seems that the same stimulus gives rise to the formation of a normal diminutive chamber in smaller specimens and to formation of a sac-like diminutive chamber in larger specimens (HEMLEBEN *et al.*, 1987).

Formation of a sac-like or a diminutive chamber precedes gamete release by 24–48 h (HEMLEBEN *et al.*, 1987). Thus the sac-like morphotype reproduces predominantly around new moon (Fig. 11C). because normalforms reproduce around full moon (BIJMA *et al.*, 1990; EREZ *et al.*, 1991), one might speculate that sac-like morphotypes [*G. sacculifer* (Brady)] and normalform morphotypes [*G. trilobus* (Reuss)] are actually subspecies that have evolved through reproductive isolation in time. If individuals begin to mate during separate time intervals (assortative mating; GOODENOUGH, 1978) so that two gamete pools are established, the stage is set for speciation. The subspecies concept could explain the

poor correlation between size and time (Fig. 9). Pre-terminal stages of sac-like and normalform morphotypes are indistinguishable and only the formation of the final chamber reveals the true identity. If their life-cycles are indeed divergent, development as a function of time is obscured. Apparently, their ontogenetic migration is identical (Fig. 8).

In the absence of any other evidence such as reproduction under controlled laboratory conditions or any ontogenetic proof (e.g. BRUMMER *et al.*, 1987), the subspecies concept remains controversial. Moreover, formation of kummersacs, predominantly around full moon, would reject the hypothesis. At this stage we therefore assume that normalforms, kummerforms, kummersacs and sac-like morphotypes represent phenotypes of one species. Apparently, reproduction in the first three phenotypes is synchronized by the same *Zeitgeber* (around full moon) whereas the sac-like phenotypes undergo gametogenesis outside the main reproductive period. It remains tempting to speculate that differential timing of the reproduction cycle could be an important mechanism for speciation in planktic foraminifers. The *G. bulloides–G. falconensis* plexus (e.g. MALMGREN and KENNETT, 1977), *G. siphonifera* type I and II (FABER *et al.*, 1988, 1989), and *G. ruber* white and pink may have evolved this way. For speculation on what triggers reproduction, SPINDLER *et al.* (1979), CARON *et al.* (1981), BIJMA *et al.* (1990) and EREZ *et al.* (1991) may be consulted.

4.6. *Biocoenosis, flux and thanatocoenosis*

The discrepancy between the living population, the settling assemblage and the sedimentary record cannot be readily explained because:

(1) the productive zone contains mostly living specimens in the process of growth, progressively more in smaller size fractions;

(2) empty specimens in the flux zone may dissolve, again, progressively more in the smaller size fractions, but the water is supersaturated with respect to calcite;

(3) differential settling speed. The decrease in mean and median diameter towards deeper intervals may be explained by differential settling speed, whereby larger specimens disappear faster from a certain horizon than smaller specimens (Table 5). This effect is more pronounced in the larger size fraction (>500 μm), as the residence time of the smaller size fractions is much longer;

(4) winnowing can be excluded because of the presence of equivalent grain sizes.

The sediment record suggests that all specimens reach maturity and reproduce. However, the high mortality of specimens <366 μm (Fig. 2B) shows that most die prior to reproduction and should therefore be abundant in the sediment. However, juveniles are largely missing in the sediment, but adults of small species such as "*Globorotalia*" *anfracta* (Parker, *Turborotalita clarkei* (Roegl and Bolli), *Globoturborotalita rubescens* Hofker, and *Globoturborotalita tenella* (Parker), are present. The observation of CARON *et al.* (1990) that specimens with GAM-calcification dissolve slower than specimens without, would indicate dissolution. However, aragonitic pteropods are abundant in the sediment.

The presence of empty non-gametogenic shells in the water column shows that the cytoplasm of dead shells can be removed quickly without dissolving the test. Such shells are present in the water column at a depth of 500 m but not in the sediment recovered from 600 m depth. We therefore assume that dissolution does not take place in the water column but may occur at the sediment–water interface before complete burial. In contrast to our

Table 6. Percentage of each morphotype in the flux assemblage (100–500 m depth) and in the sediment as a function of size

Size class	<366		366–448		448–556		556–683		>683	
	Flux	Sediment	Flux	Sediment	Flux	Sediment	Flux	Sediment	Flux	Sediment
NOR	100	100	81	77	79	63	74	50	36	38
SAC	0	0	9	20	7	24	21	39	46	43
KUM	0	0	5	3	0	11	0	7	0	12
KUMSAC	0	0	5	0	14	2	5	4	18	7

findings, REISS and HALICZ (1976) observed immature specimens in the sediments of the Gulf of Elat/Aqaba.

From laboratory experiments we know that the formation of kummerform or sac-like morphotypes is followed by gametogenesis, with more or less GAM-calcification (HEMLEBEN *et al.*, 1987). *Globigerinoides sacculifer* in the sediment is enriched with respect to sac-like and kummerform morphotypes, especially in the 448–683 μm fraction, compared to specimens from 100 to 500 m depth (Table 6, Fig. 12). Although, sac-like chambers are normally formed in the larger size fractions, their enrichment in the sediment is most conspicuous in the smaller fraction. In contrast, the kummerforms which are normally formed in the smaller fraction of the standing stock, are particularly enriched in the larger size fractions in the sediment (Table 6). Although, we are not able to solve this paradox, one must remember that the flux assemblage represents only a moment whereas the sediment surface (0–0.5 cm) may combine the populations of up to 1000 years. More work should be carried out in order to solve these contradicting observations.

5. CONCLUSIONS

(1) Three zones can be distinguished in the water column. An upper, productive zone, where growth and development takes place. An intermediate, small zone where reproduction takes place, and a large flux zone with gametogenetic and dead shells on their way to the ocean floor.

(2) *Globigerinoides sacculifer* reproduces around full moon and at approximately 80 m depth (probably in the chlorophyll maximum). Most premature specimens die and sink to the ocean floor, but some ascend to the surface. After less than 18 days they reach the surface and are approximately 100 μm in diameter. From *ca.* 200 μm onwards, they descend within 9–10 days to the reproduction depth and undergo gametogenesis.

(3) The definition of the morphotypes is based on shape and relative size of the terminal chambers. Two basic morphotypes are defined by shape, namely normalform and sac-like. Two secondary morphotypes are distinguished by the relative size of the terminal chamber, kummerform and kummersac, respectively.

(4) Mature normalform specimens reproduce around full moon. Most kummerform and kummersac morphotypes are formed just prior to full moon and reproduce simultaneous with the normalform morphotypes. Sac-like specimens, on the other hand, are abundant around new moon and represent individuals that undergo gametogenesis outside the period of main reproduction.

(5) Comparison of the size and morphotype distribution in the flux assemblage and in the sediment suggests that selective dissolution may take place at the water–sediment interface, or that yet unknown processes are involved.

Acknowledgements—Master and crew of the FS *Meteor* and the cruise leaders H. Thiel (Leg two) and H. Weikert (Leg five) are gratefully acknowledged for excellent cooperation. We further want to thank M. Rolke (Leg two) and A. Auras (Leg five) for shipboard assistance, D. Mühlen and G. Höckh for help in sample analysis and measurement and H. Hüttemann for SEM operation. J. E. van Hinte, J. D. Milliman, K. M. Towe, J. Ottens and an anonymous reviewer are acknowledged for their valuable criticism and comments. For the generous consent to use their multiple open and closing gear we want to thank H. Weikert and J. Lenz. The financial support of the DFG (SPP Meteorauswertung, He 697/7) is thankfully acknowledged.

REFERENCES

ALMOGI-LABIN A. (1984) Population dynamics of planktic Foraminifera and Pteropoda—Gulf of Aqaba, Red Sea. *Proceedings Koninklijke Nederlandse Akademie van Wetenschappen.*, Serie. B, **87**(4), 481–511.

AURAS-SCHUDNAGIES A., D. KROON, G. GANSSEN, CH. HEMLEBEN and J. E. VAN HINTE (1989) Distributional pattern of planktonic foraminifers and pteropods in surface waters and top core sediments of the Red Sea, Gulf of Aden and western Arabian Sea, controlled by the monsoonal regime and other ecological factors. *Deep-Sea Research*, **36**, 1515–1533.

BÉ A. W. H. (1980) Gametogenic calcification in a spinose planktonic foraminifer, *Globigerinoides sacculifer* (Brady). *Marine Micropaleontology*, **5**, 283–310.

BIJMA J., J. EREZ and CH. HEMLEBEN (1990) Lunar and semi-lunar reproductive cycles in some spinose planktonic foraminifers. *Journal of Foraminiferal Research*, **20**(2), 117–127.

BIJMA J., CH. HEMLEBEN and K. WELLNITZ (1993) Lunar-influenced carbonate flux of the planktic foraminifer *Globigerinoides sacculifer* (Brady) from the central Red Sea. *Deep-Sea Research*, **41**, 511–530.

BRUMMER G. J. A., CH. HEMLEBEN and M. SPINDLER (1987) Ontogeny of extant spinose planktonic foraminifera (Globigerinidae): A concept exemplified by *Globigerinoides sacculifer* (Brady) and *G. ruber* (d'Orbigny). *Marine Micropaleontology*, **12**, 357–381.

CARON D. A., A. W. H. BÉ and O. R. ANDERSON (1981) Effects on the variations in light intensity on life processes of the planktonic foraminifer *Globigerinoides sacculifer* in laboratory culture. *Journal of the Marine Biological Association of the U.K.*, **62**, 435–451.

CARON D. A., O. R. ANDERSON, J. L. LINDSEY, W. W. FABER JR and E. L. LIM (1990) Effects of gametogenesis on test structure and dissolution of some spinose planktonic foraminifera and implications for test preservation. *Marine Micropaleontology*, **16**(1/2), 93–116.

EREZ J., A. ALMOGI-LABIN and S. AVRAHAM (1991) Lunar Reproduction Cycle in *Globigerinoides sacculifer* (Brady). *Paleoceanography*, **6**(3), 295–306.

FABER W. W., JR, O. R. ANDERSON, J. L. LINDSEY and D. A. CARON (1988) Algal-foraminiferal symbiosis in the planktonic foraminifer *Globigerinella aequilateralis*: I. Occurrence and stability of two mutually exclusive chrysophyte endosymbionts and their ultrastructure. *Journal of Foraminiferal Research*, **18**(4), 334–193.

FABER W. W., JR, O. R. ANDERSON and D. A. CARON (1989) Algal–foraminiferal symbiosis in the planktonic foraminifer *Globigerinella aequilateralis*: II. Effects of two symbiont species on foraminiferal growth and longevity. *Journal of Foraminiferal Research*, **19**(3), 185–193.

FAIRBANKS R. G., M. S. SVERDLOVE, R. FREE, P. H. WIEBE and A. W. H. BÉ (1982) Vertical distribution and isotopic fractionation of living planktonic foraminifera from the Panama Basin. *Nature*, **298**, 841–844.

GANSSEN G. and D. KROON (1991) Evidence for Red Sea surface circulation from oxygen isotopes of modern surface waters and planktonic foraminiferal tests. *Paleoceanography*, **6**(1), 73–82.

GOODENOUGH U. (1978) *Genetics*. Holt-Saunders, New York, 840 pp.

HALICZ E. and Z. REISS (1981) Paleoecological relations of Foraminifera in a desert-enclosed sea—The Gulf of Aqaba (Elat), Red Sea. *Marine Ecology*, **2**(1), 15–34.

HEMLEBEN CH., M. SPINDLER and O. R. ANDERSON (1989) *Modern planktonic Foraminifera*. Springer-Verlag, Berlin, 363 pp.

HEMLEBEN CH., M. SPINDLER, I. BREITINGER and R. OTT (1987) Morphological and physiological responses of *Globigerinoides sacculifer*–(Brady) under varying laboratory conditions. *Marine Micropaleontology*, **12**, 305–324.

HEMLEBEN CH., D. MÜHLEN, R. K. OLSSON and W. A. BERGGREN (1991) Surface texture and the first occurrence of spines in planktonic foraminifera from the early Tertiary. *Geologisches Jahrbuch*, **A128**, 117–146.

MALMGREN B. A. and J. P. KENNETT (1977) Biometric differentiation between recent *Globigerina bulloides* and *Globigerina falconensis* in the southern Indian Ocean. *Journal of Foraminiferal Research*, **7**(2), 130–148.

REISS Z. and E. HALICZ (1976) Phenotypy in planktonic foraminiferida from the Gulf of Elat. *Israel Journal of Earth Sciences*, **25**, 27–39.

REISS Z., B. LUZ, A. ALMOGI-LABIN, E. HALICZ, A. WINTER, M. WOLF and D. A. Ross (1980) Later Quaternary Paleoceanography of the Gulf of Aqaba (Elat), Red Sea. *Quaternary Research*, **14**, 294–308.

SCHMIDT R. (1984) Ecology of living planktonic foraminifera in the eastern caribbean near Barbados, West-Indies—a computer-intensive study. Ms Thesis, University of Tübingen.

SPERO H. J. (1987) Symbiosis in the planktonic foraminifer, *Orbulina universa*, and the isolation of its symbiotic dinoflagellate, *Gymnodinium béii* sp. nov. *Journal of Phycology*, **23**. 307–317.

SPINDLER M., CH. HEMLEBEN, U. BAYER, A. W. H. BÉ and O. R. ANDERSON (1979) Lunar periodicity of reproduction in the planktonic foraminifer *Hastigerina pelagica*. *Marine Ecology, Progress Series* 1, **1**, 61–64.

TAKAHASHI K. and A. W. H. BÉ (1984) Planktonic foraminifera: factors controlling sinking speeds. *Deep-Sea Research*, **31**, 1477–1500.

VERCH N., M. UNGEWIB, K. SCHULZE and D. QUADFASEL (1989a) MINDIK 1987–RV METEOR cruise 5. CTD observations in the Red Sea and Gulf of Äden. Technical report 1-89. (Unpublished Manuscript.)

VERCH N., M. PETZOLD, P. MAHNKE and D. QUADFASEL (1989b) Hydrographic bottle data obtained in the Red Sea and Gulf of Aden during RV METEOR cruise 5–MINDIK 1987. Technical report 2-89. (Unpublished Manuscript.)

WEBER E. (1986) *Grundriss der biologischen Statistik*. Anwendungen der Mathematischen Statistik in Forschung, Lehre und Praxis. VEB Gustav Fischer Verlag, Jena, 652 pp.

WEIKERT H. (1987) Plankton and the pelagic environment. In: *Key environments Red Sea*, A. J. EDWARDS and S. M. HEAD, editors, Pergamon Press, Oxford, pp. 90–111.

WEIKERT H. and co-workers (1988) *Berichte aus dem Zentrum für Meeres- und Klimaforschung der Universität Hamburg*. Nr. 0, expeditionsbericht, METEOR-Reise 5 Abschnitt 5, 112 pp.